ISSN 2411-3336; e-ISSN 2541-9404

JOURNAL OF MINING INSTITUTE

Zapiski Gornogo instituta

Journal homepage: pmi.spmi.ru

Research article

Peculiarities of formation, isomorphism and geochemistry of trace elements of sphalerite and wurtzite unusual varieties from the Goniatite occurrence (Pai-Khoi Ridge, Nenets Autonomous District)

Aleksandr B. Makeyev✉, Ilya V. Vikentyev, Elena V. Kovalchuk, Vera D. Abramova, Vsevolod Yu. Prokofyev

Institute of Geology of Ore Deposits, Petrography, Mineralogy and Geochemistry, RAS, Moscow, Russia

***How to cite this article*:** Makeyev A.B.,Vikentyev I.V., Kovalchuk E.V., Abramova V.D., Prokofyev V.Yu. Peculiarities of formation, isomorphism and geochemistry of trace elements of sphalerite and wurtzite unusual varieties from the Goniatite occurrence (Pai-Khoi Ridge, Nenets Autonomous District). Journal of Mining Institute. 2024. Vol. 270, p. 861-876.

Abstract

A unique Mn-, Cd-bearing sphalerite from quartz-calcite veins in the coal-bearing series (Visean C_1v) marine sediments in a 50 km segment of the middle course of the Silova-Yakha River in the Arctic zone of the European part of Russia (Pai-Khoi Ridge) has been studied. The veins have a conformable and cross-cutting occurrence in two types of rocks: gray limestones and black siliceous-carbonaceous shales, the area is known as the Goniatite occurrence. The sulfide content in vein samples ranges from 0.1 to 2 vol.%. The chemical composition of 27 monomineral samples of Mn-, Cd-bearing sphalerites was studied, 82 points were analyzed. Correlations between typomorphic elements-impurities were revealed and correlation matrix was constructed. Cu, V, Ga, In, Sn, As, Sb, Bi, Pb, Tl, Se, Ag, Au, Ni are positively correlated with each other; Cd, Mn and Ge are negatively correlated with each other. The hydrothermal fluid involved in crystallization of sphalerite is characterized by low temperature (164-211 °C) and average salinity of 5-6 wt.% eq. NaCl. An updated "portrait" of typomorphic features (composition and properties) of sphalerite of the Pai-Khoi province was obtained. The features allowing to determine the type of impurity entering the sphalerite structure – in the form of isomorphic impurity or in the form of microinclusions of paragenetic association minerals – have been established. Submicron inclusions of sulvanite and colusite, invisible by other methods, were detected in sphalerite (by LA-ICP-MS method).The cathodoluminescence data of sphalerite from the Pai-Khoi province were typified. In contrast to other provinces, ZnS crystals here are characterized by almost complete absence of isomorphic iron. This allowed us to study pure isomorphism schemes of ZnS↔MnS, ZnS↔CdS, namely cathodoluminescence and other types of luminescence. The presence of a rare wurtzite-4H polytype in assemblage with sphalerite was revealed. High contents of strategic metals Cd, Ga, In, Ge in the ZnS matrix, as well as sulvanite (V, Cu) in a single paragenesis were found. A serious reassessment of the potential for industrial use of this mineralization will be required.

Keywords

sphalerite; wurtzite; Pai-Khoi; LA-ICP-MS; trace elements; fluid; cathodoluminescence

Funding

The work was carried out within the framework of the state task of IGEM RAS N FMMN-2021-0005, the studies by LA-ICP-MS method were performed under the RNF grant N 23-17-00266.

Received: 21.06.2023 ***Accepted: 27.12.2023*** ***Online: 04.04.2024*** ***Published: 25.12.2024***

Introduction.

Natural zinc sulfides – cubic sphalerite and hexagonal wurtzite – are widespread minerals [1, 2] and informative indicators of conditions of mineral formation [3-5]. Due to simplicity of the crystal structure and diversity of formation mechanisms in a large number of rock types, many trace elements (Ag, Au, As, Bi, Cd, Co, Cu, Fe, Ga, Ge, Ge, Hg, In, Mn, Ni, Pb, Sb, Se, Te, Sn, Tl, V) can be accumulated in ZnS. In some cases, these impurities are extracted mainly from ores containing sphalerite and wurtzite (e.g., Cd, Ga, Ge, Tl). These chemical elements can exist in different chemical states: (*A*) enter the structure of sphalerite in "invisible" form as isomorphic impurity (Fe, Mn, Cd, Hg, Tl) or as nanoparticles (Ag, Au, Cu); (*B*) become part of microinclusions of some

This is an open access article under the CC BY 4.0 license

minerals (e.g., chalcopyrite, tennantite-tetrahedrite, petzite, sulvanite) in the matrix of zinc sulfides (e.g. As, Bi, Sb, Te, V). Sometimes these heterogeneous microinclusions cannot be identified in the host mineral even by the EPMA or LA-ICP-MS methods. The structural and chemical forms of some impurity elements can vary (e.g. Au, Ag, Cu, Pb, Ga, Ge) depending on the type of deposit. There are also additional difficulties associated with the occurrence of minerals characterized by the same type of structure (e.g. chalcopyrite, sulvanite, colusite) in a similar mineral paragenesis. In sphalerite and wurtzite intergrowths and sprouting zones and sectors in which some impurities accumulate in sphalerite and others in the zones composed of wurtzite are observed [6]. Understanding of physicochemical properties and oxidation degree of impurity elements in zinc sulfides helps to improve the recovery of valuable metals at mining and processing plants, which is also important from ecological point of view. In recent years, the extraction of a number of rare "critical" metals (In, Ga, Ge) has become particularly relevant, as their consumption in the world is growing dramatically. Impurities of rare and rare-earth elements, as well as spectroscopy of minerals are widely used in the assessment of geochemical environments, which allows us to study the conditions of formation of minerals of different genesis, such as diamond [7, 8], zircon [9, 10], garnet [11], beryl [12, 13] and many others.

The concentrations of the main isomorphic impurity elements in the samples of Pai-Khoi sphalerite Mn, Cd, Fe [14], as well as partially Cu and Ga were determined earlier by wet chemistry and microprobe analysis. In the present study, the list of elements determined by LA-ICP-MS was extended to 18 elements: Ag, Au, As, Bi, Cd, Cu, Fe, Ga, Ge, In, Mn, Ni, Pb, Sb, Se, Sn, Tl, V. Cobalt was analyzed but was not detected in any sample. Mercury was not quantitatively analyzed.

The objectives of this study are as follows: determination of isomorphic capacity of Pai-Khoi zinc sulfide with respect to a wide range of impurity elements, which previously were impossible to quantify; establishment of correlation relations between them and analysis of the type of occurrence (isomorphic impurity or in the form of microinclusions); identification of the dependence of impurity concentration on the composition of the host rocks; study of conditions of mineral formation and parameters of hydrothermal fluid, as well as features of cathodoluminescence of sphalerite.

Geological position and characteristics of the object of study.

The Pai-Khoi celestine-barite-fluorite-sphalerite-sulvanite formation is represented by an almost continuous series of small zinc ore occurrences and mineralization points confined to the linear zone of hydrothermal alteration of Lower Carboniferous C_1v-s limestones and systems of spearheading fractures in black clay shales stretching along the north-eastern part of the Pai-Khoi anticlinorium (Arkhangelsk region, Nenets Autonomous District). Numerous rocky outcrops of marine sedimentary calcareous-siliceous rocks are exposed in a narrow strip (several tens of meters wide) in the valleys of the Silova-Yakha, Kara, and Sopcha rivers. The rest of the sites are sodden and covered with tundra vegetation. The visible part of sulfide mineralization is confined only to these outcrops [1, 14]. Sphalerite is found in hydrothermal-metasomatic quartz-calcite veins 1-20 cm thick and 1-5 m long. It forms individual grains or aggregates (0.5-4 cm) of irregular shape or is represented by small crystals of regular shape (0.5-3 mm). Characteristic simple crystallographic forms of sphalerite are: tetrahedron {111}, pseudo-octahedron {111, 1$\bar{1}$1}, trigontritetrahedron {112}. Polysynthetic spinel law twins [111] of unusual wurtzite-like habitus are widespread [15]. In some cases, sphalerite aggregates are surrounded by thin rims of columnar calcite.

Rare crystals of wurtzite in paragenesis with sphalerite are formed by several simple crystallographic forms: hexagonal prism {1120}, pyramid {1121}, pinacoid {0001}. The same crystallographic forms are characteristic of sphalerite twins. X-ray diagrams and strokes on faces of prism and pyramid allow to identify crystals of sphalerite twins. Wurtzite is characterized by the presence of 2H

This is an open access article under the CC BY 4.0 license

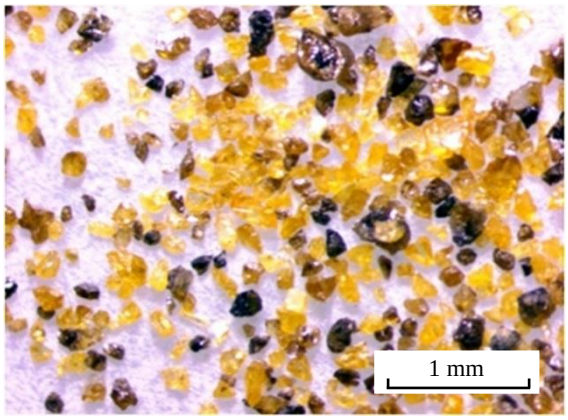


Fig.1. Monomineral fraction (sample M-454) of Cd-, Mn-sphalerite grains isolated from a quartz-calcite vein



Fig.2. Crystals of polysynthetic sphalerite twins (3C/3C'), sample B-1003 [15]

and 4H polytypes that form accretions with polysynthetic sphalerite microtwins (3C/3C′). The features of polytypy and twinning of these crystals were described in [15].

Sphalerite of the Goniatite occurrence has colours varying from light yellow to dark orange, red, brown, brownish-red and brown (Fig.1, 2). Regular brightening of sphalerite colour is observed up the section of the Visean-Serpukhov (C_1v-s) calcareous-slate strata saturated with sphalerite-bearing quartz-calcite veins. The sulfide content in the veins varies from 0.1 to 2 vol.%. Some of sphalerite crystals and grains are zonal: the inner part is dark orange and the outer part is orange-yellow. Zoning is indistinguishable in reflected light, but it is clearly visible in the dark field of the ore optical microscope, on images in the backscattered electron (BSE) mode [14]. Numerous but small in homogeneities arising from the polycrystalline structure of grains, increased content of manganese, cadmium and other impurities are clearly visible only in the cathodoluminescence mode.

Cadmium sphalerite in association with yushkinite $V_{1-x}S{\cdot}n[(Mg, Al)(OH)_2]$, fluorite and sulvanite [16, 17] often contains solid mineral and gas-liquid inclusions. Visible solid inclusions are represented by sulvanite and vein nonmetallic minerals. The size of fluid inclusions varies from 0.003 to 0.05 mm. The value of the filling factor varies within narrow limits – 0.90-0.95. The shape of gas-fluid inclusions is isometric (rounded) or in the form of well-defined negative crystals: in sphalerite the shape of negative crystals is tetrahedral or cubo-tetrahedral. Crushing of quartz-calcite veins causes a distinct hydrogen sulfide odour. The presence of nugget sulfur and hydrogen sulfide is confirmed by N.V.Sokerina, the temperature of formation of mineral association Cd-sphalerite is estimated at 120-150 °C [18].

The chemical composition of the studied sphalerite samples has noticeable features – it is dominated by varieties with an abnormally high content of manganese (up to 14.53 mol.% MnS) and cadmium (up to 3.83 mol.% CdS) and with a very low iron content – 0.01- 0.30 mol.% [14]. Crystals with high Mn and Cd content are usually represented by syntactic intergrowths of 2H and 4H wurtzite polytypes with polysynthetic sphalerite twins. Unusual impurities of V and Ni, as well as relatively high contents of Cu, Ga, Tl, Sb and Sn make this type of sphalerite an excellent object for research. The maximum concentration of impurities is noted in dark brown crystals. The high V content may be due to microinclusions of sulvanite Cu_3VS_4 or similar minerals.

The chemical composition of the studied samples is closely related to the type of host rocks [14]. Manganese-containing sphalerite is associated with black siliceous-carbonaceous-clayey shales, and cadmium-bearing sphalerite is associated with limestones. Obviously, this reflects the connection between mineral formation and the pH environment: Mn-containing sphalerite crystallized under moderately acidic conditions; on the contrary, Cd-sphalerite – under moderately alkaline conditions.

This is an open access article under the CC BY 4.0 license

Lavender-yellow Cd-sphalerite, containing up to 7.83 wt.% Cd (6.83 mol.% CdS), occurs in the northeastern part of the western flank of the Pai-Khoi anticlinorium in quartz-calcite veins among Serpukhov (C_1s) limestones of similar age and siliceous shales [16].

We attribute the Mn-, Cd-containing sphalerite with sulvanite of the Goniatite occurrence to the first (I) mineral assemblage. Limestones of different ages contain quartz-calcite veins with Cd-sphalerite, which is a member of three mineral assemblages: (II) sphalerite-sulvanite-yushkinite-fluorite (Fluorite stream, Yushkinite gorge in the upper reaches of the Silova-Yakha river basin, limestones of the Serpukhov stage C_1s, lavender-yellow sphalerite); (III) sphalerite-(sulvanite)-fahlore-V-As-germanite – (middle reaches of the Silova-Yakha River, C_2, lavender-yellow sphalerite); (IV) fluorite-galena-sphalerite (Buredan fluorite deposit, Serpukhov C_1s limestones with brown-red sphalerite) [1, 16, 19].

Cadmium-bearing sphalerite occurs in the form of transparent brownish-red or lavender-yellow isometric grains, and also exists in crystals of hexagonal habitus, which are polysynthetic twins or 6H polytypes. Characteristic features of its composition are the absence of iron and low manganese content [16]. Thus, we can observe a mechanism of direct substitution of Zn↔Cd. The variations and impurity concentrations are generally similar to Mn-bearing zinc sulfides; however, the absence of Sb and the presence of As and Ge are important indicators of this type of sphalerite. High concentrations of arsenic and germanium are very probably related to microinclusions of V-As-germanite [19].

The specific composition of the studied sphalerite affects its physical properties. The studied Cd-sphalerite exhibits photoluminescence with maximum luminescence peaks at 485-495 and 580-590 nm, which is due to the presence of copper and manganese centres. The intensity of luminescence decreases with increasing cadmium and manganese content, which is in good agreement with studies of similar materials. A prolonged phosphorescence was also observed for these samples. A less intense photoluminescence peak at 590 nm was noted for manganese sphalerite [14]. This luminescence goes out with increasing Mn concentration.

The thermoluminescence of Cd-bearing sphalerite is also specific. The maximum thermoluminescence levels are noted at 70 °C, another peak with lower intensity at 200 °C. The Cu ion replacing Zn is responsible for the appearance of electron capture centres, forbidden zone energy $E_j(70°)$ = = 0.37 eV. Analyses of thermoluminescence spectra show that this energy is transferred to the emission centres Cu (530 nm) and Mn (590 nm) Thermoluminescent properties of Mn-sphalerite are different: maximum thermoluminescence is observed at 200-210 °C and 280-320 °C, with the intensity of the second peak 3-6 times lower compared to the first peak; they are associated with the emitting Mn-centres. The total thermoluminescence level for Cd-sphalerite is 10-100 times higher than for Mn-sphalerite [14]. Any types of luminescence are not characteristic for iron-bearing zinc sulfides.

Clear correlations between chemical composition and cell parameter of the studied crystals have been established. Cd and Mn impurities lead to an increase in the cell parameter of ZnS (Mn-sphalerite: a_0 = 5.416-5.449, average 5.429 Å; Cd-sphalerite: a_0 = 5.413-5.437, average 5.420 Å), the following regression equation was calculated for ZnS with Cd, Mn, Fe impurities:

$$a_0 = 5.4083 + 0.000456X + 0.00210Y + 0.00424Z, \quad (1)$$

where X, Y, Z are the concentrations of FeS, MnS, CdS in mol.%, respectively [14].

This relationship closely corresponds to the known Skinner equation [20] for synthetic sphalerite crystals.

The influence of chemical composition on sphalerite density (D) was revealed earlier for both Mn- and Fe-bearing sphalerites. The density of Mn-ZnS (3.981-4.075 g/cm^3, average 4.040 g/cm^3) and Fe-bearing sphalerites (3.972-4.094, average 4.071 g/cm^3) is lower than the theoretical density of pure sphalerite (4.089 g/cm^3). On the contrary, the density of Cd-ZnS is higher (4.088-4.129, average 4.101 g/cm^3) [14]. The following regression equation was calculated:

$$D = 4.081 - 0.00498X - 0.00817Y + 0.00741Z, \quad (2)$$

where X, Y, Z are FeS, MnS, CdS mol.%, respectively [14].

This is an open access article under the CC BY 4.0 license

Mn- and Fe-bearing sphalerite is paramagnetic, while Cd-bearing sphalerite is diamagnetic. Therefore, the magnetic susceptibility χ of crystals from a collection of Fe- and Mn-containing sphalerite was studied [14]. The following equation relating the concentrations of these impurities and the magnetic susceptibility was proposed:

$$\chi = -0.30 + 1.10X + 1.68Y \cdot 10^{-6} \text{ cm}^3/\text{g}, \quad (3)$$

where X and Y are the concentration of Fe and Mn, %.

Thus, the chemical composition of sphalerite containing Mn, Cd and Fe can be fairly confidently calculated from its physical properties. To achieve this goal, it is necessary to solve the system of three equations (1)-(3) with three known crystallochemical and physical parameters [14].

The ZnS-MnS system was studied in hydrothermal conditions at temperatures of 300-550 °C and pressure of 500-1500 atm [14], and the ZnS-CuS system was similarly studied [21]. Based on the obtained results and literature data, isobaric (1000 atm) cross sections of the subsolidus part of the phase diagram of these systems were constructed. A single-crystal X-ray study of artificial crystals representing a mixture of sphalerite and wurtzite-2H was carried out. It was found that isomorphous admixture of manganese and copper in zinc sulfide significantly reduces the temperature of the phase transition between sphalerite and wurtzite.

Methods.

Chemical analyses of the Pai-Khoi sphalerite collection were carried out by the EPMA (JEOL JXA-8200 microanalyser equipped with five wave dispersive spectrometers) and LA-ICP-MS (Thermo XSeries 2 quadrupole mass spectrometer with New Wave UP213 laser sampling system) methods according to the standard methodology at the IGEM-Analytics collaborative centre in IGEM RAS. Microthermometric study was carried out at IGEM RAS using a measuring complex consisting of a Linkam THMSG 600 camera (England) mounted on an Olympus BX51 microscope (Japan), combined with a video camera and a control computer. The chemical composition of the fluid in the inclusions was estimated from measurements of phase transitions and transformations that occurred during heating and cooling of the polished plate. The accuracy of the temperature measurement was 0.2 °C in the temperature range from –20 to +20 °C; it decreases at higher and lower temperatures.

The composition of salts prevailing in the aqueous solutions of fluid inclusions was estimated by measuring the melting point of the eutectic [22]. The total concentration of salts in two-phase fluid inclusions was calculated from the ice melting temperature based on experimental data for the NaCl-H_2O system [23]. Salt concentrations and liquid densities were estimated using FLINCOR software [24].

Studies by the colour cathodoluminescence (CCL) method of sphalerite were carried out in the LAMV laboratory of IGEM RAS (O.M.Zhilicheva) on the X-ray microanalyser MS-46 of the "Cameca" company. The optical system of the device was upgraded and adapted to a high-resolution CCD-digital camera of "Videoscan" (Russia) model 285/C/P-USB (SONY ICX285AQ, colour, TE-cooled). Control software "Videoscan Viewer". Unlike commercially produced types of CL detectors, the proposed scheme developed in Glaukon OOO (Russia) allows to obtain images of cathodoluminescence in real colours and subject them to further mathematical processing. Luminescence excitation in the samples was carried out by electron beam irradiation in vacuum at room temperature. CCL registration was carried out in the screen mode at an accelerating voltage of 20 kV and a current of 25 nA. The exposure time of one frame in the scanning mode was 240 s. Due to the constructive limitation of the imaging area and to achieve stability of the probe characteristics, it is possible to register either individual small grains or a consecutive series of frames of larger extractions with a window of 300 × 350 μm. The preparations were sputtered with a thin layer of carbon.

The advantage of the cathodoluminescence facility at IGEM RAS is the possibility of using two wave spectrometers for phase identification in the (BSE) mode and direct visualization of the CCL colour at the point of electron probe incidence.

Cathodoluminescence. One of the features of Mn- and Cd-bearing sphalerites is intense cathodoluminescence. This characteristic and well-known property of manganese-cadmium sphalerites is never

This is an open access article under the CC BY 4.0 license

observed in iron-rich varieties. In grains of manganese-cadmium sphalerite cathodoluminescence in orange and orange-brown luminescence is intensely manifested over the entire surface, and bright orange only in some parts of the crystal. The intensity of cathodoluminescence decreases with increasing Mn content.

The cathodoluminescence of sphalerite crystals from quartz-calcite veins in four mineral associations of the Pai-Khoi province was studied in order to typify sphalerite by colour and reveal its internal structure: (I) Orange, yellow, brown colouredsphalerite from Mn-, Cd-bearing sphalerite-wurtzite-sulvanite-quartz-calcite association in limestones and schists of Visean age (C_1v) – Goniatite occurrence; (II) Lavender-yellow sphalerite of Cd-sphalerite-sulvanite-yushkinite-fluorite-quartz-calcite association in limestones of Serpukhov (C_1s) age [16, 17]; (III) lavender-yellow sphaleritefrom Cd-sphalerite-(sulvanite)-fahlore-V, As-germanite-quartz-calcite association in limestones of Middle Carboniferous (C_2) age; (IV) red sphalerite from Cd-sphalerite-chouleite-galenite-fluorite-quartz-calcite association in limestones of Buredan occurrence of Serpukhov age (C_1s). The chemical composition of polished preparations of sphalerite (Table 1) was analyzed by the microprobe.

Table 1

Normalized chemical composition (EPMA) of a representative sample of sphalerite and wurtzite of the Pai-Khoi anticlinorium (for the study by CCL method), wt.%

Samples	Association	Zn	Mn	Cd	Fe	S	Sum
M-443	I	62.91	2.26	2.06	0.01	32.76	100.0
M-446	– " –	59.66	5.50	1.82	0.02	33.00	100.0
M-457a	– " –	58.83	6.11	2.05	0.01	33.00	100.0
M-462g	– " –	62.50	2.24	2.57	0.02	32.67	100.0
M-464	– " –	61.53	3.70	1.84	0.07	32.86	100.0
M-410	II	63.38	0.21	4.03	0.02	32.36	100.0
M-431	III	64.64	0.33	2.43	0.01	32.59	100.0
M-415	IV	66.44	0.07	0.64	0.03	32.82	100.0

We obtained 160 CCL and 150 BSE images of grains and crystals of 14 sphalerite samples, including two samples of high-iron sphalerite (with 6.7-7.2 wt.% Fe), in which no CCL was shown. Manganese-cadmium sphalerites of the first (I) mineral association of the Goniatite occurrence (Fig.3) possess bright orange-brown CL luminescence caused by isomorphic manganese centres. The internal structure of crystals is expressed by: sectorial structure, growth zones with different concentration of impurities, twinning bands and zones composed of 2H, 4H wurtzite polytypes, as well as inclusions of vein minerals (quartz and calcite). Calcite has its own red-orange luminescence and often forms thin rims (up to 10-30 μm) of columnar-fibrous structure around sphalerite grains. Quartz does not glow and appears in the obtained images as a black structureless field.

Crystals and grains of cadmium sphalerite of all three other mineral associations have homogeneous composition and do not possess noticeable features of internal structure, and the intensity of colouring of CCL is conditioned only by the thickness of preparations. However, they luminesce differently in the three colours. Cd-sphalerite (II) of the mineral association has a very bright blue luminescence (Fig.4), and sphalerite (III) of the mineral association has a bright green luminescence (Fig.5 *a*, *b*), which may be due to the corresponding impurities (centres) entering the crystal structure in accordance with the following heterovalent isomorphism schemes: $Cu^{+} + Ga^{3+} \rightarrow 2Zn^{2+}$ or $Ag^{+} + Ga^{3+} \rightarrow 2Zn^{2+}$ [14].

Cd-sphalerite crystallites (Fig.5 *c*, *d*) from the Buredan sphalerite-galenite-fluorite occurrence (IV association) have brown CCL (with Mn^{2+} and Ge^{4+} luminescence centres). The peculiarity of sphalerite of this occurrence is the presence of thin rims of chouleite around all sphalerite grains 5-10 μm thick with a green CCL.

This is an open access article under the CC BY 4.0 license

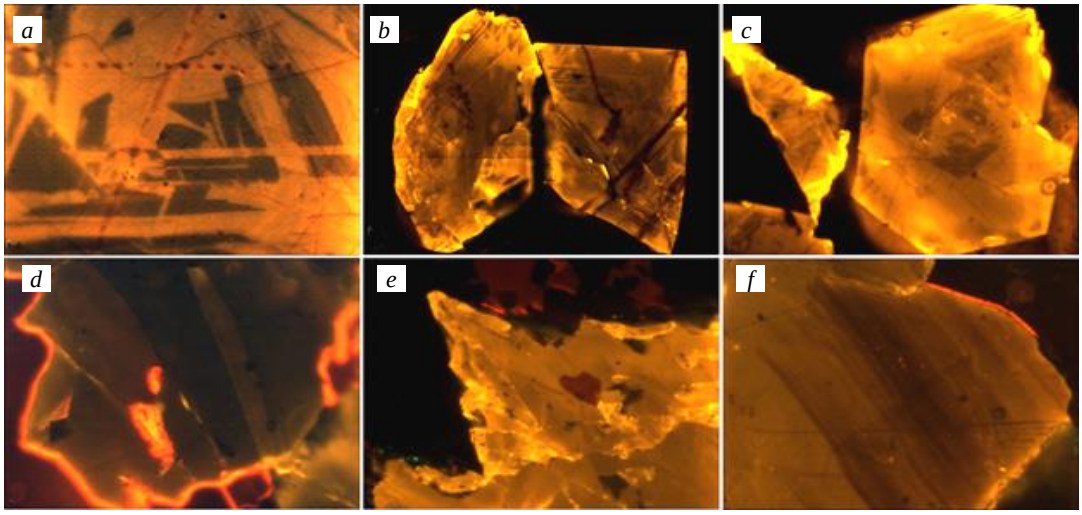


Fig.3. Orange-brown cathodoluminescence of Mn-, Cd-bearing sphalerite (*a, b, d-f*) and wurtzite (*c*) of the Goniatite occurrence. Samples: *a* – M-443, *b, c* – M-446, *d* – M-457a, *e* – M-462g, *f* – M-464. The width of all images is 350 μm

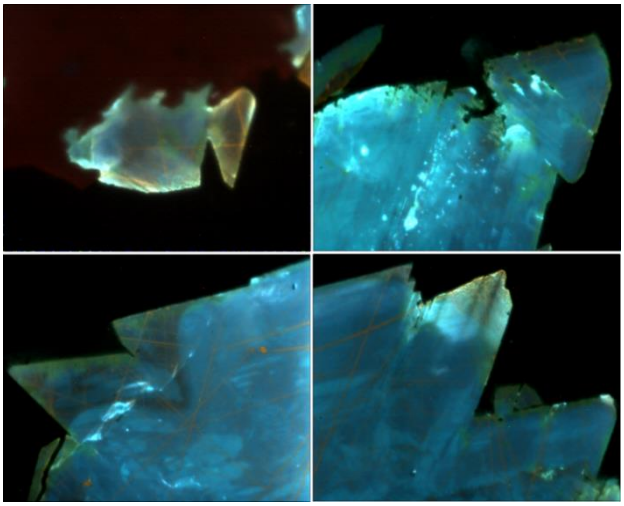


Fig.4. Blue cathodoluminescence of cadmium sphalerite from (II) mineral association, sample M-410. Image width 350 μm

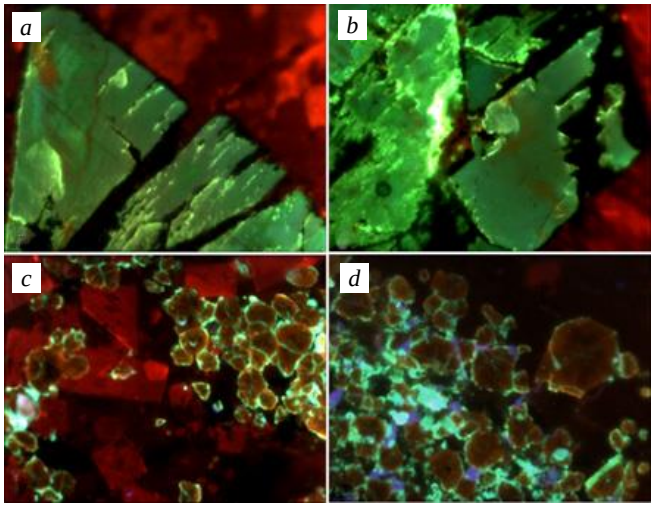


Fig.5. Green cathodoluminescence of cadmium sphalerite (*a, b*) from mineral association III, sample M-431. Brown cathodoluminescence of cadmium sphalerite (*c, d*) from mineral association IV, sample M-415. Calcite glows red, fluorite – violet, chouleite (CdS) – green, quartz (black) has no luminescence

Trace elements in sphalerite and wurtzite. Twenty-seven samples (82 analysis points) were studied by the LA-ICP-MS method. The analyses were performed both in point (in the centre, in the middle and along the outer edge of grains) and linear (profile ablation) modes (Fig.6). The profile ablation mode was used to study the distribution of minor trace elements in grains. The distribution of all studied elements in different grains of the same sample is homogeneous. At the same time, significant variations were noted in the compositions of several grains of a number of samples. The results of studies of chemical composition of sphalerite of Goniatite occurrence and their statistical processing are presented in Tables 2-5. In Tables 2 and 3 the results of chemical analyses are given only partially (in Table 2 – 14 samples, 42 points of analyses; in Table 3 – 9 samples, 27 points of analyses). Due to the large amount of information, only the most representative samples were selected for publication on the grounds of diversity and breadth of sampling variation. The statistical sampling (Tables 4, 5) includes all analyzed samples: Mn, Cd-ZnS – 13 samples, 43 analyses (from shales); Cd, Mn-ZnS – 14 samples, 39 analyses (from limestones). In addition, we expected to find monomineral zones and crystal sections composed only of sphalerite and only of wurtzite, with

This is an open access article under the CC BY 4.0 license

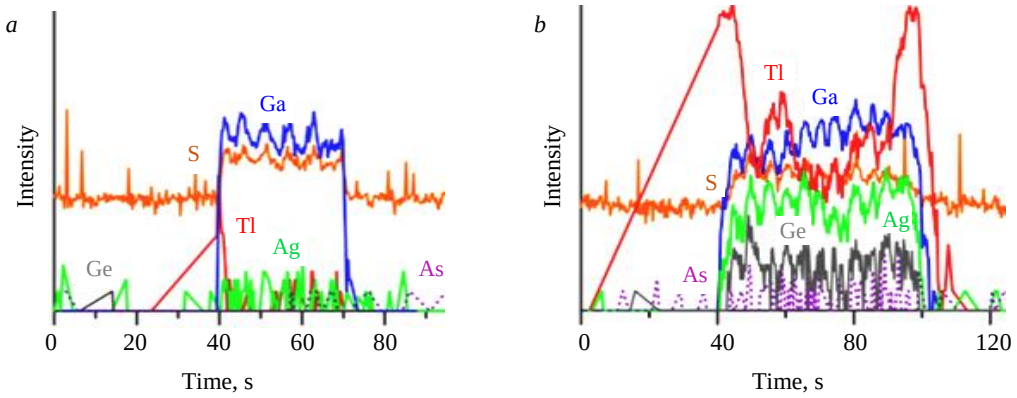


Fig.6. Typical LA-ICP-MS spectra of composition distribution of Pai-Khoi Mn-, Cd-sphalerites along the grain profile: *a* – yellow sphalerite (M-454) without impurities of paragenetic minerals; *b* – brown sphalerite (M-455) with visually invisible sulvanite (colusite?) ingrowth. Fluctuations of S and impurity elements (Tl, Ga, Ge, As, Ag) contents were revealed. The size of the zone of increased isomorphic contents of S, Ga, Ag is 30 μm, inclusion is 50 μm

different capacities with respect to impurity elements. However, without the involvement of local X-ray diffraction studies, it has not yet been possible to do so. Manganese sphalerite has relatively higher isomorphic capacity with respect to many elements: Fe, In, Ga, Se, Au, Ni, As. Cadmium sphalerite has relatively higher isomorphic capacity with respect to Ge, Tl, Sb, Sn, V.

Table 2

EPMA analyses of zinc sulfide of the Goniatite occurrence, wt.%

Sample number	Average composition (2σ)					Colour of sphalerite grains Intervening rock
	Zn	Mn	Cd	S	Sum	
M-453	64.43 0.17	1.60 0.07	1.16 0.02	32.84 0.11	100.03	Brown limestone
M-454	63.27 0.29	1.41 0.05	2.71 0.14	32.62 0.17	100.01	Yellow and brown limestone
M-455	63.37 0.30	1.28 0.05	2.76 0.05	32.6 0.09	100.01	Brown limestone
M-456	62.72 0.18	2.49 0.85	2.02 0.28	32.78 0.04	100.01	Brown limestone
M-458a	62.29 0.20	1.83 0.02	3.26 0.19	32.56 0.15	99.94	Brown limestone
M-459a	63.66 0.26	1.25 0.03	2.40 0.12	32.65 0.13	99.96	Yellow limestone
M-459-2	63.71 0.28	1.25 0.03	2.32 0.17	32.66 0.17	99.94	Yellow limestone
M-463	61.55 0.25	3.67 0.16	1.83 0.09	32.88 0.27	99.93	Red-orange black slates
M-709	63.84 0.24	1.22 0.16	2.29 0.18	32.66 0.11	100.01	Brown limestone
M-713	62.33 0.16	2.47 0.13	2.46 0.11	32.72 0.16	99.98	Yellow and brown limestone
M-719	60.26 0.34	4.98 0.21	1.80 0.11	32.97 0.21	100.01	Brown black slates
M-720	62.66 0.23	1.86 0.12	2.83 0.08	32.63 0.12	99.98	Brown limestone
M-732	63.73 0.15	1.02 0.05	2.67 0.08	32.6 0.14	100.02	Brown limestone
M-734	61.38 0.26	3.71 0.20	2.02 0.16	32.86 0.21	99.97	Orange and brown black shale

This is an open access article under the CC BY 4.0 license

Table 3

Chemical composition of Pai-Khoi sphalerite samples (Goniatite occurrence) according to LA-ICP-MS data (27 analysis points), g/t

Sample number	Content of impurity elements in sphalerite (mean±2σ), minimum-maximum values								
	Mn (1)	Cd (3)	Fe (3)	In (0.1)	Ga (0.1)	Ge (0.4)	Tl (0.02)	Ag (0.3)	Se (4)
M-453	16100±3300 14000-17700	14900±500 14600-15000	56±22 43-68	8.2±3.9 5.4-10.1	238±37 218-255	1.4±0.7 Bdl-1.7	0.84±0.73 Bdl -1.51	1.5±1.2 0.2-2.8	60±22 76-533
M-454	14700±150 14600-14900	34500±4800 27400-38000	150±42 123-174	13.6±1.3 12.1-14.8	457±39 404-486	1.3±0.7 Bdl-2.0	0.97±0.73 0.09-1.75	1.7±0.9 1.12-2.1	308±81 256-343
M-455	13100±2800 11800-14600	24300±700 23700-25000	197±64 169-232	17.0±3.7 14.9-18.2	717±363 508-835	16.6±3.0 14.7-18.7	56.04±38.67 16.30-91.70	64.5±21.6 52.2-72.3	218±154 51-348
M-456	41400±6200 39600-43200	15000±4000 13700-17300	122±89 79-168	7.2±2.7 6.1-8.7	277±55 250-313	5.1±0.1 5.0-5.2	2.92±1.34 1.85-4.11	5.16±2.15 4.47-6.4	32±22 20-42
M-709	11300±1200 11000-12000	19000±2600 17800-20400	58±30 43-73	8.4±2.8 7.0-9.8	599±107 493-737	2.1±0.9 1.0-3.3	3.27±0.79 2.52-4.10	4.4±2.8 1.4-7.2	61±11 55-66
M-719	46400±10500 43200-52400	10700±3000 9100-12100	181±82 134-207	9.6±5.6 7.12-8.6	479±81 398-571	10.1±6.8 2.4-17.7	2.69±1.07 1.72-3.86	4.8±4.1 Bdl-8.6	475±244 226-690
M-721	15200±3700 13800-17300	16800±1500 16000-17500	120±21 109-130	10.7±3.7 8.8-12.4	500±152 338-652	9.2±6.5 1.3-16.5	2.17±0.73 1.81-2.54	25.1±19.0 3.0-44.4	113±37 93-130
M-732	10400±800 10000-10800	21200±3700 17500-24800	166±45 147-191	9.1±1.8 8.2-10.0	321±191 226-417	1.8±1.7 Bdl-3.6	8.20±5.14 2.11-13.70	2.4+1.4 0.7-4.0	335±75 292-361
M-734	40100±7600 35900-44700	14400±2300 13300-15500	153±75 110-178	22.1±12.4 16.5-29.8	632±308 371-917	1.6±1.3 0.7-3.0	2.11±0.72 1.60-2.45	8.3±5.8 Bdl-15.1	74±6 69-81

Sample number	Content of impurity elements in sphalerite, minimum-maximum values								
	Cu (8)	Au (0.04)	Ni (0.6)	As (1.8)	Sb (0.06)	Bi (0.02)	Pb (0.04)	Sn (0.2)	V (0.1)
M-453	243-572	Bdl-0.21	Bdl	Bdl	Bdl-0.47	Bdl-0.53	1.09-2.27	0.5-26.6	Bdl-22.6
M-454	467-511	Bdl-0.53	1.0-2.1	Bdl	0.23-0.52	0.03-1.00	1.22-1.97	1.2-11.6	Bdl-5.0
M-455	2290-2780	0.02-0.49	1.0-2.9	8.3-12.9	52.90-82.90	0.16-0.41	1.41-2.89	281-427	174.0-235.0
M-456	455-749	Bdl-0.65	0.4-2.1	2.2-8.7	5.63-17.40	0.08-0.56	0.95-1.73	33.5-74.5	22-51.3
M-709	635-1073	Bdl	Bdl-1.1	Bdl-3.3	2.90-18.90	0.07-0.28	0.86-1.22	8.7-54.8	9.4-51.5
M-719	700-1074	Bdl-0.21	Bdl-1.1	Bdl-3.1	3.30-8.50	0.28-1.22	0.83-1.49	18.5-125	12.9-89.0
M-721	504-2013	0.34-0.63	Bdl-1.1	1.5-6.2	5.22-50.80	0.12-0.63	0.73-1.06	30.7-323	16.7-199.0
M-732	289-641	0.12-1.20	1.0-1.5	1.9-3.4	0.32-5.52	0.23-0.82	1.03-2.33	2.4-28.9	1.2-21.4
M-734	408-1020	0.05-2.50	Bdl-10.8	Bdl-3.0	0.99-6.08	0.22-0.59	0.97-2.51	13.0-61.7	Bdl-37.1

Note. The chemical element symbol is followed by the detection limit. Samples M-455 and M-721 contain thin emulsion phenocrysts of sulvanite (Cu_3VS_4); samples M-453, M-454, M-455, M-456, M-709, M-721, M-732 – from veins in limestone; samples M-719 and M-734 – from veins in shale. Bdl – below detection limit.

This is an open access article under the CC BY 4.0 license

Journal of Mining Institute. 2024. Vol. 270. P. 861-876

©Aleksandr B. Makeyev, Ilya V. Vikentyev, Elena V. Kovalchuk, Vera D. Abramova, Vsevolod Yu. Prokofyev, 2024

This is an open access article under the CC BY 4.0 license

Journal of Mining Institute. 2024. Vol. 270. P. 861-876

©Aleksandr B. Makeyev, Ilya V. Vikentyev, Elena V. Kovalchuk, Vera D. Abramova, Vsevolod Yu. Prokofyev, 2024

Table 4

Correlation matrix of Pai-Khoi sphalerite composition (82 points of analyses)

Elements	Mn	Cd	Fe	In	Ga	Ge	Tl	Ag	Se	Cu	Au	Ni	As	Sb	Bi	Pb	Sn	V
Mn	1	–0.531	0.137	0.331	–0.022	–0.170	–0.220	–0.136	0.408	–0.179	0.204	0.045	0.496	–0.280	0.113	0.066	–0.272	–0.188
Cd	–0.531	1	–0.063	–0.089	0.132	0.089	0.166	0.119	–0.040	0.205	–0.211	–0.102	–0.188	0.254	–0.208	0.011	0.268	0.148
Fe	0.137	–0.063	1	–0.007	–0.069	0.020	0.024	–0.009	0.050	–0.017	0.059	0.057	0.008	–0.025	–0.016	0.013	–0.011	–0.017
In	0.331	–0.089	–0.007	1	0.665	0.018	0.079	0.012	–0.090	0.302	0.391	–0.110	0.134	0.131	0.045	0.151	0.133	0.051
Ga	–0.022	0.132	–0.069	0.665	1	0.067	0.326	0.327	–0.236	0.701	0.060	–0.097	0.031	0.499	–0.112	–0.116	0.555	0.395
Ge	–0.170	0.089	0.020	0.048	0.067	1	0.056	0.037	0.011	0.100	–0.015	–0.036	–0.068	0.094	–0.040	–0.090	0.100	0.079
Tl	–0.220	0.166	0.024	0.079	0.326	0.056	1	0.233	0.072	0.463	–0.061	–0.045	0.056	0.579	–0.062	–0.017	0.497	0.353
Ag	–0.136	0.119	–0.009	0.012	0.327	0.037	0.233	1	–0.059	0.518	0.035	0.301	0.253	0.503	–0.057	0.012	0.553	0.451
Se	0.408	–0.040	0.050	–0.090	–0.236	0.011	0.072	–0.059	1	–0.059	0.065	0.021	0.368	–0.106	0.107	0.114	–0.127	0.071
Cu	–0.179	0.205	–0.017	0.302	0.701	0.100	0.463	0.518	–0.059	1	–0.007	–0.086	0.234	0.854	–0.103	–0.035	0.929	0.895
Au	0.204	–0.211	0.059	0.391	0.060	–0.015	–0.061	0.035	0.065	–0.007	1	0.144	0.265	–0.042	0.490	0.439	–0.083	–0.112
Ni	0.045	–0.102	0.057	–0.110	–0.097	–0.036	–0.045	0.301	0.021	–0.086	0.144	1	0.172	–0.067	0.130	0.113	–0.070	–0.075
As	0.496	–0.188	0.008	0.134	0.031	–0.068	0.056	0.253	0.368	0.234	0.265	0.172	1	0.276	0.292	0.367	0.194	0.248
Sb	–0.280	0.254	–0.016	0.131	0.499	0.094	0.579	0.503	–0.106	0.854	–0.042	–0.067	0.276	1	–0.095	–0.019	0.925	0.732
Bi	0.113	–0.208	0.113	0.045	–0.112	–0.040	–0.062	–0.057	0.107	–0.103	0.490	0.13	0.292	–0.095	1	0.436	–0.112	–0.123
Pb	0.066	0.011	0.113	0.151	–0.116	–0.090	–0.017	0.012	0.114	–0.035	0.439	0.113	0.367	–0.119	0.436	1	–0.012	–0.080
Sn	–0.272	0.268	–0.011	0.133	0.555	0.100	0.497	0.553	–0.127	0.929	–0.083	–0.070	0.194	0.925	–0.112	–0.012	1	0.812
V	–0.188	0.148	–0.017	0.051	0.395	0.079	0.353	0.451	0.071	0.895	–0.112	–0.075	0.248	0.732	–0.123	–0.080	0.812	1

Note. The intensity of the colouring of the cells shows an increase in the degree of correlations.

Table 5

Statistical parameters of composition of Pai-Khoi sphalerites, g/t

Indicator	*T*, °C	Components (min & max)																	
		Mn	Cd	Fe	In	Ga	Ge	Tl	Ag	Se	Cu	Au	Ni	As	Sb	Bi	Pb	Sn	V
Number of points	48	82	82	82	82	82	82	82	82	82	82	82	82	82	82	82	82	82	82
Sample $n = 27$	min	9550	9060	27	2.68	144.5	0.14	0.05	0.17	46	185	0.01	0.28	1.18	0.07	0.02	0.73	0.33	0.05
	max	62800	38000	1680	53	952	362	91.7	254	690	3060	34.3	210	17.9	82.9	52	7.13	436	390
Average indicators	157.2	31267	17632	154.3	12.16	402.2	7.70	3.44	12.87	263.0	724.0	1.44	6.74	6.40	7.84	2.11	2.17	49.5	38.9
Mn, Cd-ZnS	167.4	45724	14658	180.4	14.89	415.0	2.76	0.93	12.62	308.7	669.5	2.21	10.91	8.04	4.81	2.25	2.19	29.1	32.8
Cd, Mn-ZnS	147.7	16105	20752	127.0	9.29	388.8	12.88	6.07	13.14	215.0	781.2	0.64	2.37	4.69	11.01	1.95	2.15	70.9	45.3

Note. Orange-red Mn, Cd-ZnS sphalerite is confined to shales, and yellow-brown Cd, Mn-ZnS is confined to limestones. Manganese sphalerite has relatively large isomorphic capacity with respect to Fe, In, Ga, Se, Au, Ni, As. Cadmium sphalerite has a relatively large isomorphic capacity with respect to Ge, Tl, Sb, Sn, and V. Temperature calculated from geothermometer [6]. Samples with very high vanadium content showed unrealistic values, so data from only 48 samples are considered.

Table 4 presents the results of correlation analysis of the total sample for all (n = 82) observation points. Threshold value r = 0.14, with 95% confidence interval. The following elements are positively correlated with each other: Cu, V, Ga, In, Sn, As, Sb, Bi, Pb, Tl, Se, Ag, Au, Ni; negatively to them – Cd, Mn and Ge. For a part of elements pair correlation is not established. The first set of impurity elements tends both isomorphous incorporation into zinc sulfide and formation of microinclusions of various chalcogenides: sulvanite, colusite, renierite, stannite, fahlore and others. The second combines isomorphic elements-impurities.

All studied samples were characterized by low Fe content, varying from 43 to 293 g/t. This is characteristic of low-temperature varieties of zinc sulfide and corresponds to the light colour of its crystals, Au content is below 2.5 g/t, Ni usually does not exceed 10 g/t, but often below their detection limits.

The most important feature of zinc sulfides of the Pai-Khoi anticlinorium is the presence of V in their chemical composition. It should be reminded that sulvanite is a paragenetic mineral in the described mineral association. The ratio of sulvanite : sphalerite ≈ 1 : 10. Grains and cubic crystals of sulvanite 0.5-2 mm in size are present in each sample. To a visually controlled monomineral quality, these two minerals are fairly "cleanly" separated in the concentrate by magnetic separation (as sulvanite is diamagnetic). Sample M-455 shows maximum V content (up to 235 g/t). It also attracts attention with slightly higher concentrations (g/t) compared to the other samples: Ge 14.7-18.7; In 8.2-14.9; Cu 2290-2780; Ag 52-72.3; As 8.3-12.9; Sb 52.9-82.9; Tl 16.3-91.7. In addition, it is less homogeneous compared to other samples. This fact can be explained by the presence of tiny submicron inclusions of sulvanite – Cu_3VS_4 and colusite group minerals – $Cu_{26}V_2(As, Sn, Sb)_6S_{32}$ in the sphalerite matrix (Fig.6). These inclusions are invisible even with scanning electron microscopy. Sulvanite and colusite have a close structure, consisting of the same elements, which could be incorporated into the sphalerite structure, forming the same type of inclusions in it. The only difference is the value of the unit cell parameter. Moreover, both sulvanite and colusite are marked in ore occurrences of the province by their own mineral phases [19]. The same regularities can be found in other samples, except for yellow-coloured samples of sphalerite M-453 and M-454. Concentrations of all impurities in these samples are 10 times lower in comparison with sulvanite- and colusite-bearing ZnS grains. Thus, samples with numbers M-453 and M-454 represent "pure" monomineral zinc sulfide without solid microinclusions.

Some elements prefer to accumulate in sphalerite and wurtzite as inclusions of separate minerals. The ratio of antimony and arsenic contents (Sb > As) is the same in all samples. The maximum value of C_{Sb} antimony concentration is 82.9 g/t. In some cases, $C_{Sb} > C_{As}$ by a factor of 5-10, see, for example, sample M-721 (Table 3), in which C_{As} ranges from 1.5 to 6.2 g/t and C_{Sb} ranges from 5.2 to 50.8 g/t. Compared to other semi-metal elements. Bi content in the samples is minimal. Bismuth was not detected in light coloured ZnS grains (C_{Bi} does not exceed 1 g/t), although its concentration for dark grains is only slightly higher (up to 1.22 g/t).

In dark-coloured samples, Ge content ranges from 1 to 18.70 g/t, Ga from 277 to 917 g/t, Tl from 1.72 to 91.70 g/t, and Ag from "not detected" to 52.2 g/t. Recall that earlier [14] very high local concentrations of gallium in brown wurtzite-4H of the same province were determined using microprobe. In pure yellow-coloured sphalerite these concentrations are much lower (g/t): Ge content varied from "not detected" to 1.97, Ga from 218 to 487, Tl from "not detected" to 1.75, Ag from 0.21 to 2.75.

Fluid inclusions. Fluid inclusions were studied in preparations (polished plates of sample B-1003) made from a quartz vein with prismatic orange-red crystals (see Fig.2), composed of polysynthetic twins of manganese sphalerite from a rocky outcrop in the valley of the river Putyu, southeastern slope of the Pai-Khoi anticlinorium [15].

According to known criteria [25], primary, secondary, and mixed primary-secondary fluid inclusions were identified among fluid inclusions in quartz (Fig.7). Fluid inclusions that are uniformly

This is an open access article under the CC BY 4.0 license

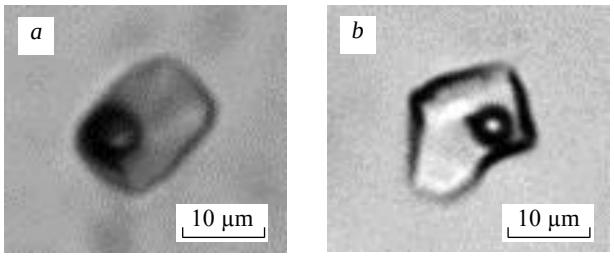


Fig.7. Primary (*a*) and primary-secondary (*b*) two-phase fluid inclusions in quartz in accretion with sphalerite (ZnS-Mn)

distributed throughout the host mineral or related to growth zones are primary. Inclusions confined to cracks cutting the host mineral are considered secondary. Primary-secondary fluid inclusions are confined to cracks that do not reach the outer boundaries of crystals and grains. Their composition in terms of phase filling is close to primary inclusions. In sphalerite crystals, a few analogous fluid inclusions of a similar phase composition were found – two-phase gas-liquid inclusions of water-salt solutions. Due to the intense color of sphalerite, it turned out to be impossible to conduct thermo-cryometric studies, so the same primary inclusions in paragenetic quartz were chosen for the study. They are evenly distributed throughout the volume of the quartz grain. The parameters of phase transitions were obtained from primary-secondary inclusions. Secondary inclusions were not studied. The close paragenesis of these two minerals (ZnS and quartz) is proven by the presence of induction surfaces of joint growth.

Table 6 shows the results of thermo- and cryometric studies of individual fluid inclusions in quartz intergrown with sphalerite. The ore-forming fluid contained predominantly sodium chloride (NaCl). This is evidenced by the eutectic temperatures of inclusion solutions (from –22 to –21 °C). Two-phase gas-liquid inclusions in quartz (Fig.7) homogenize into liquid at temperatures from 164 to 211 °C. Salt concentration varies from 5.2 to 6.1 wt.% eq. NaCl. The density of the liquid is 0.90-0.95 g/cm^3.

Table 6

Results of thermo- and cryometric studies of fluid two-phase gas-liquid inclusions in quartz in paragenesis with sphalerite

Inclusion type	*n*	Temperature homogenization, °C	Temperature eutectic,°C	Temperature melting, °C	Concentration, wt.% eq. NaCl	Density, g/sm^3
Primary	3	211	–21	–3.8	6.1	0.90
Primary	3	196	–21	–3.9	6.2	0.92
Primary-secondary	3	182	–22	–3.2	5.2	0.93
Primary-secondary	4	164	–22	–3.8	6.1	0.95

Thus, the hydrothermal fluid from which sphalerite crystallized was characterized by a relatively low temperature (164-211 °C) and average salinity.

Discussion of results.

One of the objectives of the study was to determine the degree of monomineralisation of zinc sulfide crystals and to establish the nature and type of distribution of impurity elements in them. The greatest amount of microimpurities is characteristic of dark-coloured varieties of sphalerite (brown, dark red), and the areas with inclusions of wurtzite polytypes 2H and 4H are also confined to them [15]. Perhaps, a reliable enough way to distinguish the samples with microinclusions of sulvanite from monomineral “pure” ZnS is the presence of intercorrelating impurities of Cu, V, As, and As was not detected in samples M-453 and M-454, although “traces” of V were found in them, but only up to 22.6 g/t. Probably chalcophilic behavior of vanadium should be connected with low level of oxygen fugacity and with participation of bituminous materials in the studied mineral-forming hydrothermal system [1]. Due to the absence of As admixture it is possible to distinguish Mn-, Cd-sphalerite samples, conditionally “pure” – in contrast to ZnS grains with inclusions of other micron-sized minerals (with noticeable As admixture).

The statistical analysis of the samples (see Table 3) shows that C_{Pb} concentration is clearly not related to mineral microinclusions. Lead correlates only with Au, As and Bi. It is known that high concentrations of Pb and Sb are noted in sphalerite from Bosnia and Herzegovina [26]; researchers assume their probable isomorphic incorporation into the structure of sphalerite. Although it is also known that Pb is an isomorphous impurity in stibiocolusite [27]. The hypothesis about the presence

This is an open access article under the CC BY 4.0 license

of microinclusions of tin minerals in sphalerite is indirectly confirmed by wide variations of Sn in all samples. The maximum amount of Sn is contained in brown grains of zinc sulfide of sample M-455 (281-427 g/t), but it is also observed in yellow ZnS. There are known reports about isomorphic form of tin occurrence in sphalerite [28, 29].

The discussion of the forms of incorporation of Ge, Ga, Tl. and Ag in ZnS is a more difficult task. High concentrations of these elements can be explained both by substitution mechanisms and by the presence of individual minerals as microinclusions [30-32]. It is believed that Ag, Ga, Ge and Tl are characteristic elements for low-temperature environments of mineral formation [31-33]. However, these same elements are found in colusite group minerals: germanite and renierite with wide variations of compositions. In addition, germanite $(Cu, Ag, Tl)_{26}Fe_2(As, Sn, Ge, Sb, Bi, Ga)_6S_{32}$ often contains V [34, 35], and renierite $(Cu, Zn)_{11}Fe_4(Ge, As, Ga, Sb, Bi)_2S_{16}$ often contains Pb.

A significant isomorphic capacity of sphalerite with respect to indium and gold has been experimentally proven [36]. A more significant isomorphic incorporation of Au into sphalerite is promoted by trivalent iron and indium in heterovalent substitution mechanism.

Variations in the concentrations of Ga, In, Tl, on the one hand, and Ag, Au, Cu, on the other hand, are interconnected, and they probably enter sphalerite according to the heterovalent scheme of isomorphism $(Ga^{3+}, Tl^{3+}, In^{3+}) + (Cu^{+}, Ag^{+}, Au^{+}) \leftrightarrow 2Zn^{2+}$ [33, 36, 37]. At the same time, the same elements can be directly incorporated into colusite, sulvanite, and renierite. These circumstances do not allow us to unambiguously determine the nature of these impurities.

The concentration of In is also very informative [31, 38, 39]. Indium varies insignificantly in the composition of all samples studied by us, because usually In is not clearly included in the structure of sulvanite, colusite, germanite, renierite, stannite and other minerals, but, most likely [40], is in isomorphous form. Ga, Ge and Tl were considered as typical isomorphic impurity elements in the structure of zinc sulfides [29, 31, 32].

It is interesting to note that the existence of chemically bound form of Au in sphalerite is associated with its insignificant concentration in the "invisible" form in pyrite, arsenic pyrite and sphalerite: from 120 to 300 g/t in the Iranian deposit Zarshuran [41, 42].

Rare reports of arsenic in sphalerite [43], for example, in the Alcoran mine (Chile) and selenium [44] – in the Baccu Locci deposit (Sardinia), confirm our assumptions about the possible isomorphic form of their incorporation into sphalerite.

According to the study [18], the crystallization temperature of cadmium sphalerite from the same quartz-calcite Pai-Khoi veins in association with yushkinite is somewhat lower – 120-150 °C. The results of calculation of probable crystallization temperatures of manganese-cadmium sphalerites using the Frenzel geothermometer [45], presented in Table 5, are in good agreement with these experimental data. According to these data, high-manganese sphalerite from quartz-calcite veins localized in black shales crystallized from the fluid at a higher temperature (167 °C on average) than cadmium-manganese sphalerite, which is present in veins localized in grey limestones, where it crystallized at a lower temperature (147 °C on average).

Conclusion.

We have characterized typomorphic features (composition and properties) of low-temperature zinc sulfide of the Pai-Khoi province. Impurity elements in Pai-Khoi sphalerite – Mn, Cd, Fe, Ga, Ge, Ge, Tl, Au, In, Ni, Au, Te, Se – enter the structure of ZnS mainly isomorphically. However, our data show that many impurities (Ag, Cu, Pb, V, As, Sb, Bi, Sn, Ge) can be found in sphalerite and wurtzite grains in the form of submicroscopic (which are sometimes even invisible when using the EPMA method) inclusions of sulvanite, colusite group minerals and others. Apparently, a distinctive feature of sulvanite- and colusite-bearing ZnS is a higher content of Cu, V, and As in grains. Thus, As was not detected in the "pure" samples of Mn, Cd-ZnS (M-453 and M-454), but minimal values of V (up to 22.6 g/t) were noted in the yellow varieties, which may indicate insignificant isomorphic entry of vanadium into the sphalerite composition. Thus, the noticeable As content is an important criterion for dividing ZnS samples into "pure", on the one hand, and those containing sulvanite and colusite as inclusions, on the other hand.

This is an open access article under the CC BY 4.0 license

The list of minerals forming accretions with sphalerite can be significantly expanded due to improved analytical techniques and methods of analysis. Further studies by the EBSD method will be aimed at revealing zones in crystals composed of hexagonal ZnS-wurtzite to compare them with sphalerite sites; analysis of the chemical composition of these zones will allow to additionally characterizing the "capacity" of these minerals concerning impurity elements.

The conducted studies allowed us to typify sphalerite occurrences of four mineral associations of the Pai-Khoi anticlinorium based on the colour of cathodoluminescence and the internal structure of crystals. Crystals of Mn-, Cd-sphalerite have a characteristic internal structure (sectoriality, zonality, twinning, polytypism) and orange-brown CCL. Crystals of Cd-sphalerite of other three associations have no peculiarities of internal structure, but possess typomorphic colour of the CCL: blue, green and brown.

High contents of strategic metals Cd, Ga, Ge, In in ZnS matrix, as well as in sulvanite (V, Cu) in a single paragenesis with sphalerite were established. This sulfide mineralization in quartz-calcite veins belongs to the ores easily enriched by gravity and magnetic separation. The Goniatite occurrence is likely to require a major reassessment of the potential for commercial exploitation of this mineralization.

The authors thank O.M.Zhilicheva for assistance in cathodoluminescence studies of sphalerite and wurtzite crystals. The research used the equipment of IGEM RAS (*Center for Collective Use* "*IGEM-Analitika*").

REFERENCES

1. Yushkin N.P., Eremin N.I., Makeyev A.B., Petrov T.G. Sphalerite of the Paikhoi-Yuzhnonovozemelskaya province – topominerology and typomorphism. *Trudy Institutag eologii Komi filial Akademii nauk SSSR. Problemy regionalnoi mineralogii*. 1978. Iss. 24, p. 23-52. (in Russian).

2. Cook N.J., Ciobanu C.L., Pring A. et al. Trace and minor elements in sphalerite. *Geochimica et Cosmochimica Acta*. 2009. Vol. 73. Iss. 16, p. 4761-4791. DOI: 10.1016/j.gca.2009.05.045

3. Cugerone A., Cenki-Tok B., Chauvet A. et al. Relationships between the occurrence of accessory Ge-minerals and sphalerite in Variscan Pb-Zn deposits of the Bossost anticlinorium. French Pyrenean Axial Zone: Chemistry, microstructures and ore-deposit setting. *Ore Geology Reviews*. 2018. Vol. 95, p. 1-19. DOI: 10.1016/j.oregeorev.2018.02.016

4. Frenzel M., Hirsch T., Gutzmer J. Gallium, germanium, indium, and other trace and minor elements in sphalerite as a function of deposit type – A meta-analysis. *Ore Geology Reviews*. 2016. Vol. 76, p. 52-78. DOI: 10.1016/j.oregeorev.2015.12.017

5. Lockington J.A., Cook N.J., Ciobanu C.L. Trace and minor elements in sphalerite from metamorphosed sulphide deposits. *Mineralogy and Petrology*. 2014. Vol. 108. Iss. 6, p. 873-890. DOI: 10.1007/s00710-014-0346-2

6. Pring A., Wade B., McFadden A. et al. Coupled Substitutions of Minor and Trace Elements in Co-Existing Sphalerite and Wurtzite. *Minerals*. 2020. Vol. 10. Iss. 2. N 147. DOI: 10.3390/min10020147

7. Vasilev E.A. Defects of diamond crystal structure as an indicator of crystallogenesis. *Journal of Mining Institute*. 2021. Vol. 250, p. 481-491. DOI:10.31897/PMI.2021.4.1

8. Vasilev E.A., Kriulina G.Yu., Garanin V.K. Thermal history of diamond from Arkhangelskaya and Karpinsky-I kimberlite pipes. *Journal of Mining Institute*, 2022. Vol. 255, p. 327-336. DOI: 10.31897/PMI.2022.57

9. Skublov S.G., Rumyantseva N.A., Li Q. et al. Zircon Xenocrysts from the Shaka Ridge Record Ancient Continental Crust: New U-Pb Geochronological and Oxygen Isotopic Data. *Journal of Earth Science*. 2022. Vol. 33. Iss. 1, p. 5-16. DOI: 10.1007/s12583-021-1422-2

10. Levashova E.V., Mamykina M.E., Skublov S.G. et al. Geochemistry (TE, REE, Oxygen) of Zircon from Leucogranitesof the Belokurikhinsky massif, Gorny Altai, as Indicator of Formation Conditions. *Geochemistry International*. 2023. Vol. 61. Iss. 13, p. 1323-1339. DOI: 10.1134/S001670292311006X

11. Stativko V.S., Skublov S.G., Smolenskiy V.V., Kuznetsov A.B. Trace and rare-earth elements in garnets from silicate-carbonate formations of the Kusa-Kopan complex (Southern Urals). *Lithosphere*. 2023. Vol. 23. N 2, p. 225-246 (in Russian). DOI: 10.24930/1681-9004-2023-23-2-225-246

12. Gavrilchik A.K., Skublov S.G., Kotova E.L. Trace Element Composition of Beryl from the Sherlovaya Gora Deposit. South-Eastern Transbaikalia, Russia. *Zapiski Rossiiskogo mineralogicheskogo obshchestva*. 2021. Vol. 150. N 2, p. 69-82 (in Russian). DOI: 10.31857/S0869605521020052

13. Skublov S.G., Gavrilchik A.K., Berezin A.V. Geochemistry of beryl varieties: comparative analysis and visualization of analytical data by principal component analysis (PCA) and t-distributed stochastic neighbor embedding (t-SNE). *Journal of Mining Institute*. 2022. Vol. 255, p. 455-469. DOI:10.31897/PMI.2022.40

14. Makeyev A.B. Isomorphism manganese and cadmium in sphalerite. Leningrad: Nauka, 1985, p. 128 (in Russian).

15. Makeyev A.B., Tauson V.L. On the possible genesis of some ZnS polytypes (according to a study of Pai-Khoi sphalerites). Kristallokhimiya i strukturnaya mineralogiya. Leningrad: Nauka, 1979, p. 18-25 (in Russian).

This is an open access article under the CC BY 4.0 license

16. Makeyev A.B., Pavlov L.V. A new cadmium variety of sphalerite. *Doklady Akademii nauk SSSR*. 1977. Vol. 236. N 1, p. 208-211 (in Russian).

17. Makeyev A.B., Evstigneeva T.L., Troneva N.V. et al. Yushkinit, $V_{1-x}S{\cdot}n[(Mg,Al)(OH)_2]$ – a new hybrid mineral. *Mineralogicheskii zhurnal*. 1984. Vol. 6. N 5, p. 91-98 (in Russian).

18. Sokerina N.V., Kovalchuk N.S., Isaenko S.I., Sokerin M.Y. Conditions of the Formation of Unique Mineralization with Yushkinite$V_{1-x}S{\cdot}n[(Mg,Al)(OH)_2]$ in Quartz–Calcite Veins, Pai-Khoi Ridge: Evidence from Study of Fluid Inclusions. *Doklady Earth Sciences*. 2020. Vol. 492. Iss. 2, p. 411-414. DOI: 10.1134/S1028334X20060197

19. Yushkin N.P., Makeyev A.B. Arsenic minerals of the Paikhoi-Yuzhnonovozemelskaja province. *Trudy Instituta geologii Komi filial Akademii nauk SSSR. Geologiya i poleznye iskopaemye Severo-Vostoka SSSR*. 1978. Iss. 27, p. 79-84 (in Russian).

20. Skinner B.J. Unit-cell edges of natural and synthetic sphalerites. *American Mineralogist*. 1961. Vol. 46. N 11-12, p. 1399-1411.

21. Tauson V.L., Makeyev A.B., Akimov V.V., Paradina L.F. Distribution of copper in zinc sulfide minerals. *Geokhimiya*. 1988. N 4, p. 492-505 (in Russian).

22. Borisenko A.S. Cryometric technique applied to studies of the saline composition of solution in gaseos fluid inclusions in minerals. *Russian Geology and Geophysics*. 1977. N 8, p. 16-27.

23. Bodnar R.J., Vityk M.O. Interpretation of microthermometric data for H_2O-NaCl fluid inclusions. Fluid Inclusions in Minerals: Methods and Applications. Blacksburg: Virginia Tech, 1994, p. 117-130.

24. Brown P.E. FLINCOR: a microcomputer program for the reduction and investigation of fluid-inclusion data. *American Mineralogist*. 1989. Vol. 74. N 11-12, p. 1390-1393.

25. Redder E. Fluid inclusions in mineral. Vol. 1. The nature of inclusions and methods for their study. Moscow: Mir, 1987. p. 557 (in Russian).

26. Radosavljević S.A., Stojanović J.N., Radosavljević-Mihajlović A.S., Vuković N.S. (Pb–Sb)-bearing sphalerite from the Čumavići polymetallic ore deposit. Podrinje Metallogenic District, East Bosnia and Herzegovina. *Ore Geology Reviews*. 2016. Vol. 72. Part 1, p. 253-268. DOI: 10.1016/j.oregeorev.2015.07.008

27. Spiridonov E.M., Badalov A.S., Kovachev V.V. Stibiocolusitis $Cu_{26}V_2(Sb,Sn,As)_6S_{32}$: a new mineral. *Doklady Akademii nauk SSSR*. 1992. Vol. 324. N 2, p. 411-414 (in Russian).

28. Evrard C., Fouquet Y., Moëlo Y. et al. Tin concentration in hydrothermal sulphides related to ultramafic rocks along the Mid-Atlantic Ridge: a mineralogical study. *European Journal of Mineralogy*. 2015. Vol. 27. N 5, p. 627-638. DOI: 10.1127/ejm/2015/0027-2472

29. Voudouris P., Repstock A., Spry P.G. et al. Physicochemical constraints on indium-, tin-, germanium-, gallium-, gold-, and tellurium-bearing mineralizations in the Pefka and St Philippos polymetallic vein- and breccia-type deposits, Greece. *Ore Geology Reviews*. 2021. Vol. 140. N 104348. DOI: 10.1016/j.oregeorev.2021.104348

30. Rambaldi E.R., Rajan R.S., Housley R.M., Wang D. Gallium-bearing sphalerite in a metal-sulfide nodule of the Qingzhen (EH3) chondrite. *Meteoritics & Planetary Science*. 1986. Vol. 21. Iss. 1, p. 23-31. DOI: 10.1111/j.1945-5100.1986.tb01223.x

31. Paradis S. Indium. germanium and gallium in volcanic- and sediment-hosted base-metal sulphide deposits. Symposium on Critical and Strategic Materials Proceedings, 13-14 November 2015, Victoria, British Columbia. British Columbia Geological Survey Paper 2015-3, p. 23-29.

32. Xiong Y. Hydrothermal thallium mineralization up to 300 °C: A thermodynamic approach. *Ore Geology Reviews*. 2007. Vol. 32. Iss. 1-2, p. 291-313. DOI: 10.1016/j.oregeorev.2006.10.003

33. Paiement J.-P., Beaudoin G., Paradis S., Ullrich T. Geochemistry and Metallogeny of Ag-Pb-Zn Veins in the Purcell Basin, British Columbia. *Economic Geology*, 2012. Vol. 107. N 6, p. 1303-1320. DOI: 10.2113/econgeo.107.6.1303

34. Spiridonov E.M., Kachalovskaya V.M., Badalov A.S. Varieties of colusite, about vanadium and vanadium-arsenic "germanite". *Vestnik Moskovskogo universiteta. Seriya 4. Geologiya*. 1986. Iss. 3, p. 60-69 (in Russian).

35. Spiridonov E.M. On the composition of germanite. *Doklady Akademii nauk SSSR*. 1987. VOL. 295. N 2, P. 477-481 (IN RUSSIAN).

36. Tonkacheev D.E., Chareev D.A., Abramova V.D. et al. The substitution mechanism of Au in In-, Fe- and In-Fe-bearing synthetic crystals of sphalerite, based on the data from EPMA and LA-ICP-MS study. *Lithosphere*. 2019. Vol. 19. N 1, p. 148-161 (in Russian). DOI: 10.24930/1681-9004-2019-19-1-148-161

37. Huston D.L., Sie S.H., Suter G.F. et al. Trace elements in sulfide minerals from eastern Australian volcanic-hosted massive sulfide deposits; Part I. Proton microprobe analyses of pyrite, chalcopyrite, and sphalerite, and Part II. Selenium levels in pyrite; comparison with $\delta^{34}S$ values and implications for the source of sulfur in volcanogenic hydrothermal systems. *Economic Geology*. 1995. Vol. 90. N 5, p. 1167-1196. DOI: 10.2113/gsecongeo.90.5.1167

38. Ishihara S., Hoshino K., Murakami H., Endo Y. Resource Evaluation and Some Genetic Aspects of Indium in the Japanese Ore Deposits. *Resource Geology*. 2006. Vol. 56. Iss. 3, p. 347-364. DOI: 10.1111/j.1751-3928.2006.tb00288.x

39. Johan Z. Indium and germanium in the structure of sphalerite: an example of coupled substitution with Copper. *Mineralogy and Petrology*. 1988. Vol. 39. Iss. 3-4, p. 211-229. DOI: 10.1007/BF01163036

40. Filimonova O.N., Trigub A.L., Tonkacheev D.E. et al. Substitution mechanisms in In-, Au-, and Cu-bearing sphalerites studied by X-ray absorption spectroscopy of synthetic compounds and natural minerals. *Mineralogical Magazine*. 2019. Vol. 83. Iss. 3, p. 435-451. DOI: 10.1180/mgm.2019.10

41. Asadi H.H., Voncken J.H.L., Hale M. Invisible gold at Zarshuran. Iran. *Economic Geology*. 1999. Vol. 94. N 8, p. 1367-1374. DOI: 10.2113/gsecongeo.94.8.1367

42. Filippov V.A., Ryabinin V.F., Syzoeva Z.Z. The Gagarka gold deposit in the central Urals. Russia. *Geology of Ore Deposits*. 2013. Vol. 55. N 1, p. 27-40. DOI 10.1134/S1075701513010030

43. Clark A.H. Arsenian sphalerite from Mina Alcarán, Pampa Larga, Copiapó, Chile. *American Mineralogist*. 1970. Vol. 55. N 9-10, p. 1794-1797.

This is an open access article under the CC BY 4.0 license

44. Pirri I.V. On the occurrence of selenium in sulfides of the ore deposits of Baccu Locci (Gerrei, SE Sardinia). *Neues Jahrbuchfür Mineralogie*. 2002. Vol. 5, p. 207-224. DOI: 10.1127/0028-3649/2002/2002-0207

45. Frenzel M., Voudouris P., Cook N.J. et al. Evolution of a hydrothermal ore-forming system recorded by sulfide mineral chemistry: a case study from the Plaka Pb–Zn–Ag Deposit, Lavrion, Greece. *Mineralium Deposita*. 2022. Vol. 57. Iss. 3, p. 417-438. DOI: 10.1007/s00126-021-01067-y

***Authors*: Aleksandr B. Makeyev,** *Doctor of Geological and Mineralogical Sciences, Leading Researcher, abmakeev@mail.ru. https://orcid.org/0000-0001-8815-0959* (*Institute of Geology of Ore Deposits, Petrography, Mineralogy and Geochemistry, RAS, Moscow, Russia*). **Ilya V. Vikentyev,** *Doctor of Geological and Mineralogical Sciences, Chief Researcher, https://orcid.org/0000-0001-9133-7562* (*Institute of Geology of Ore Deposits, Petrography, Mineralogy and Geochemistry, RAS, Moscow, Russia*). **Elena V. Kovalchuk,** *Junior Researcher, https://orcid.org/0000-0002-6522-8212* (*Institute of Geology of Ore Deposits, Petrography, Mineralogy and Geochemistry, RAS, Moscow, Russia*), **Vera D. Abramova,** *Junior Researcher, https://orcid.org/0000-0002-7021-5272* (*Institute of Geology of Ore Deposits, Petrography, Mineralogy and Geochemistry, RAS, Moscow, Russia*). **Vsevolod Yu. Prokofyev,** *Doctor of Geological and Mineralogical Sciences, Head of Laboratory, https://orcid.org/0000-0001-7134-2655* (*Institute of Geology of Ore Deposits, Petrography, Mineralogy and Geochemistry, RAS, Moscow, Russia*).

The authors declare no conflict of interests.

This is an open access article under the CC BY 4.0 license